EURASIP Journal on Wireless Communications and Networking

RESEARCH Open Access

Improving power efficiency in 6G wireless communication networks through reconfigurable intelligent surfaces for different phase information

Amin Mahmoudi Rad[1*], Jafar Pourrostam[1] and Mohammad Ali Tinati[1]

*Correspondence:
a.mahmoudi98@ms.tabrizu.ac.ir

[1] Department of Electrical & Computer Engineering, University of Tabriz, Tabriz, Iran

Abstract

With increasing needs for high-bitrate, ultra-reliability, spectral efficiency, power efficiency, and reducing latency in the wireless network, global studies on the sixth generation of this network began in 2020. In this paper, we will look at intelligent reconfigurable surface structure and its application in new promising physical layer technologies, such as terahertz communications and UM-MIMO systems, to support very high-bitrate and superior network capacity in the 6G wireless communications. However, terahertz communications and UM-MIMO systems are the primary research points and confront many challenges for practical implementation. They require many RF chains and create problems in terms of cost and hardware complexity which RIS can simplify hardware and reduce cost. Therefore, we will present different modeling of wireless communication systems based on RIS for different phase information. Simulation results obtained by examining SNR performance and the error probability that shows the improvement of the received signal quality. According to results, RIS-based wireless communications can become an optimized model for future wireless communication systems.

Keywords: Power efficiency, RIS, 6G wireless network, Phase information, SNR, BER

1 Introduction

The development of the Fifth Generation (5G) wireless communication standard, which reached its peak between 2017 and 2019, followed by the global deployment of these networks, is expected to lead by increasement in data transmission rate, the bandwidth of wireless networks, ultra-reliable services with low latency and also, supporting an extreme coverage in large number of networks connection. However, the primary 5G standard brings more flexibility to system design which completed in 2018 using millimeter-waves and the Orthogonal Frequency Division Multiplexing (OFDM) method. Researchers are constantly finding emerging technology applications for the Beyond Fifth Generation (B5G), including Non-Orthogonal Multiple Access (NOMA), Visible Light Communication (VLC), Ultra-Massive-Multiple-Input-Multiple-Output (UM-MIMO) systems, terahertz communications, and new technologies for designing

antennas [1, 2]. Even if the future technologies of the Sixth Generation (6G) look like their counterparts at this time, the new applications used and the recent network trends in 2030 may make communication engineering and design more challenging [3, 4]. In this paper, we will look at the potential technology of Reconfigurable Intelligent Surfaces (RIS) in 6G wireless communications, which represents some basic improvements in the physical layer, whether it is the control of the propagation path or the communication wireless channel to increase the Quality of Service (QoS) in the new generations of wireless systems. Many emerging technologies, such as UM-MIMO systems and terahertz communications, are considered as promising technologies to support very high access speed and optimal network capacity in 6G wireless communication systems [5, 6]. However, such technologies still face many challenges for practical implementation. In particular, extremely large multi-input-multiple-output systems and terahertz communications require a very large number of Radio-Frequency (RF) chains, resulting in problems in terms of hardware cost and complexity [7, 8].

In Sect. 2, we will introduce new method that is investigated to solve the above problems, which is done by using the powerful capabilities of reconfigurable surfaces in changing electromagnetic waves [9, 10]. By investigating an effective and promising method in future wireless communication systems that are also tunable, two futuristic models using these reconfigurable surfaces explained, which are RF Chain-Free (FRCF) transmitter and Space Down-Converter (SDC) receiver [11, 12].

In Sect. 3, we will introduce a new wireless transmission system based on RIS for different phase information [13, 14], by expressing the proposed RIS-SDC and RIS-RFCF methods. In other words, these surfaces are intelligent systems that control the propagation environment [15, 16]. It should note that the concept of RIS-based transmissions is quite different from Multiple-Input-Multiple-Output (MIMO) systems and beamforming methods. On the other hand, RIS has many tiny, inactive elements that only reflect the transmitted signal by tunable phase change without a separate power supply for computing, decoding, encryption, or retransmission at the RF level [17, 18]. The concept of intelligent surfaces was introduced as one of the first works by using active frequency selectors to improve signal coverage. It is a suitable alternative to the beamforming method that requires many antennas [19]. We will model wireless transmission systems based on configurable smart surfaces and check their mathematical relationships. Also, the quality of the received signal can increase by tuning the phase change of each element in RIS [20]. Utilizing the entire continuous surface in RIS-based wireless communication has led to the evolution of UM-MIMO systems [21]. We present a model for bit error rate (BER) performance analysis using moment generating function in RIS-based wireless communication systems for different phase information and draw exciting results depending on different types of signal-to-noise ratio (SNR) [22]. Based on the promising functionality of RIS-based wireless communication, we will use it as an RFCF transmitter, in which phase-shift reflectors were used not only to maximize SNR but also to transmit data [23].

In Sect. 4, after examining the simulation of the proposed models in terms of SNR performance and error probability, it can be concluded that the proposed wireless transmission methods based on reconfigurable intelligent surfaces improve power consumption to achieve a certain error probability and improve power efficiency. If we

have information on the wireless channel, low SNR values and a small number of passive elements which form RIS could be used. In wireless communication modelling, it will achieve optimum power efficiency and high reliability. Computer simulations have shown that RIS can be used efficiently as a SDC reflector and an RFCF transmitter in futurity 6G wireless communication systems.

In Sect. 5, we can conclude from the general point of view in this paper, we will be explaining the basis of RIS work in two models, RIS-RFCF and RIS-SDC, so that our research can be completed as mentioned in [21]. It is shown that, if we do not have the wireless channel information in these two models, it will still be more power efficient than when RIS did not operate on Rayleigh's wireless channel. A wireless communications system with excellent power efficiency and high reliability, near zero error probability, can also be achieved in a consciously transmission mode by selecting the right number of RIS passive elements.

2 Methods

As shown in Fig. 1, there are two types of RIS: reflective and transmissional. In reflective-type RIS, the radiated electro-magnetic (EM) wave is converted into a reflected wave, in which case the amplitude and phase of this wave are adjusted by external control signals, and on the contrary, in the transmission-type RIS, the radiated electromagnetic wave becomes it mainly turns into a transmitted wave [6].

N is the number of RIS elements. For example, in the reflective-type, assuming that E_i is a parameter, which determines the relationship between the transmission medium and the impedance discontinuity. That is equal to the correlation coefficient between the radiation wave and the reflection wave from each element, as well as, $A_i(\phi_i)$ and ϕ_i represent the controllable amplitude and phase change, respectively. Also, E_i and $\widetilde{E}_i$ are the parameters of the radiation wave and the reflection wave of this element [24]. The relationship between E_i and $\widetilde{E}_i$ can express as:

$$\widetilde{E}_i = A_i(\phi_i) \cdot e^{j\phi_i} \cdot E_i \tag{1}$$

$\widetilde{E}(p)$ is the total EM wave reflected at the observation point p in front of RIS, so that is the result of combining all the reflected waves from all of these elements, which depends

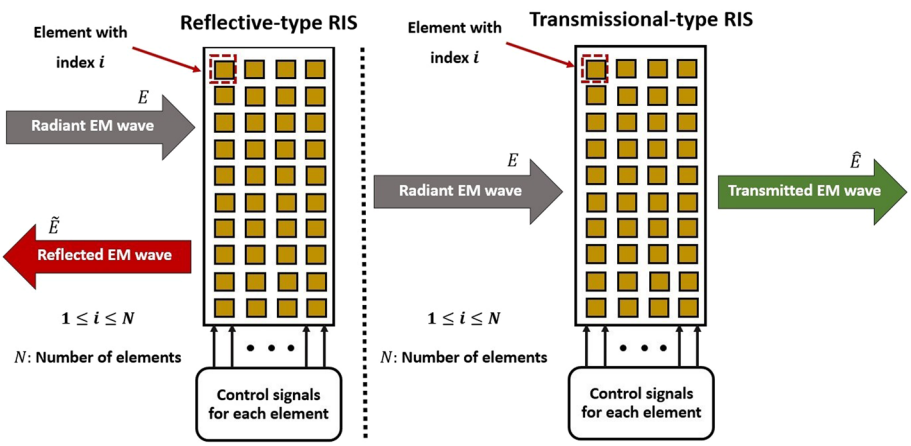

Fig.1 Reflective-type RIS and transmissional-type RIS patterns

on the parameter $h_i(p)$. That is the frequency response of wireless channel between each element and the observation point, so it can write as follows:

$$\widetilde{E}(p) = \sum_{i=1}^{N} h_i(p) \cdot \widetilde{E}_i = \sum_{i=1}^{N} h_i(p) \cdot A_i(\phi_i) \cdot e^{j\phi_i} \cdot E_i \tag{2}$$

This equation indicates the working principles of RIS structure of the reflection-type, and the counterpart of the transmissional-type $\widehat{E}_i$ has similar regulations. But instead, with the difference in the transmissional-type, the transmitted EM wave changes [25]. Taking advantage of the superior capability of RIS to apply passive EM wave changes with less complex hardware, we offer two new wireless communication architectures: RIS-based RFCF wireless transmitter and RIS-based SDC wireless receiver. Both methods have good potential for reducing hardware costs and complexity in futurity UM-MIMO and terahertz communications. Essentially, RISs are composed of two-dimensional thin-film microwave structures with intelligent EM attributes, which can use in a wide range of operating frequencies, from microwaves to visible light [26]. Adjustable elements with metal and dielectric structures were typically used in the precise design of these surfaces. The phase and amplitude of the radiation wave to RIS can adjust by these elements. Such new architectures can reduce the cost of hardware and the complexity of wireless communications. However, these new architectures are helpful for futurity UM-MIMO systems in the terahertz band [7].

2.1 RIS-based RFCF wireless transmitter

Wireless transmitters play an essential role in modern wireless communication systems and have made great strides over the past few decades. Although, despite the rapid advancement of electronic technologies, the number of significant innovations in the architectural design of these transmitters is small. Most high-performance transmitters now rely on the traditional model. As shown in Fig. 2, each RF circuit requires a Power Amplifier (PA), two mixers, and several Low-Pass Filters (LPF) and Band-Pass Filters (BPF), which results in very high hardware complexity and power

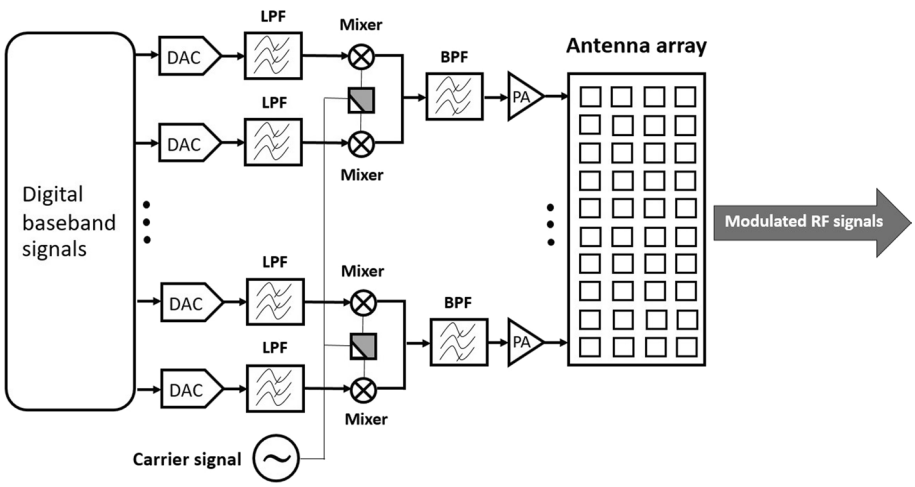

Fig.2 Traditional transmitter model

waster used in the UM-MIMO. For example, the Direct Antenna Modulation (DAM) method is proposed. Modulated RF signals were generated directly using time-varying antennas, which also simplifies the hardware design, which only supports a few less efficient base modeling schemes, such as On–Off Keying (OOK) and Frequency Shift Keying (FSK). There is another similar method to use in this architecture called Direct Phase Shifter Modulation (DPSM), which is proposed to get phase modulation through compressed design however suffers from a slow transfer rate due to the gradual update speed of the phase shift [9].

Figure 3 shows the RIS-based RFCF transmitter model, which primarily reduces the hardware complexity of UM-MIMO and terahertz communications. In this model, the single-frequency carrier signal radiates through the air channel through the antenna to the elements. The baseband signal is mapped to the control signals to adjust the reflection coefficients of the elements. The result is a modulated EM wave. For phase shift keying (PSK) modulation, it is sufficient to use RIS control signals to change the desired phases of RF signals since the amplitude and phase response of each element is controlled independently by a separate digital-to-analog converter (DAC). The suggested transmitter can now produce continuous multi-channel RF signals. As a result, advanced signal processing techniques such as space–time modulation and beamforming enable future MIMO and UM-MIMO technologies. Also, in this method, regardless of how many channels were used to control the transmission power of the signal carrying into the channel, only a narrow-band power amplifier is needed. At the same time, there is no need to use mixers and filters. Therefore, it dramatically reduces hardware complexity and execution costs. In addition, the power amplifier only needs to amplify the single-frequency carrier signal instead of the modulated broadband signal, which makes it a promising method to bypass the nonlinear matter in power amplifiers. The passive or inactive nature of RIS allows for high energy efficiency and the use of new applications, and the physical structure of the thin surface benefits from heat dissipation. So, the RF chain-free transmitter effectively reduces hardware costs, reduces power consumption, and simplifies the integration process [11].

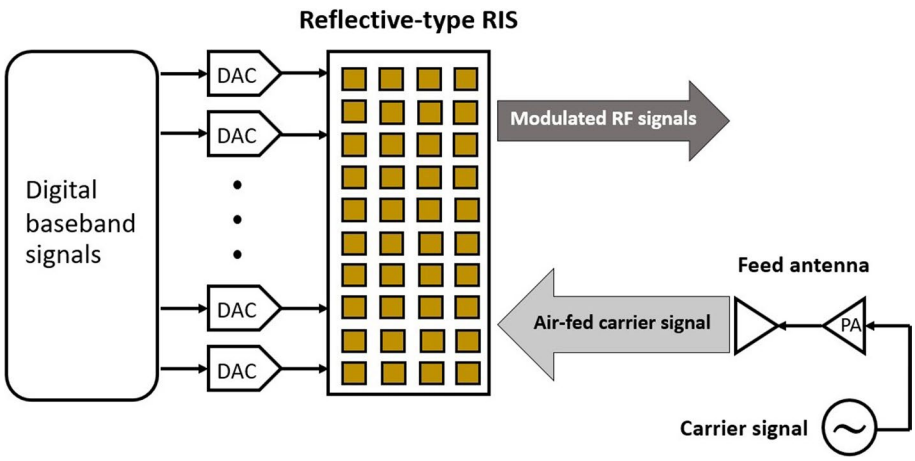

Fig.3 RIS-based RFCF transmitter model

2.2 RIS-based SDC wireless receiver

Since the EM wave passes through the RIS, its central frequency changes by $1/T_{\mathrm{RIS}}$ (T_{RIS} is the time required to change the linear phase of 2π). Because this reduction was achieved in space, it defines as space down-conversion. This method works like down-conversion mixers in a traditional receiver. Because only one RIS is used in the proposed receiver, it is simpler and more efficient than previous examples. E is the radiated wave to RIS, and $\widehat{E}$ is the transmitted wave from the RIS. The relationship between E and $\widehat{E}$ can express as:

$$\widehat{E} = e^{j\omega_{\Delta} t} \cdot E = e^{j\left(\frac{2\pi}{T_{RIS}}\right)t} \cdot E \tag{3}$$

Figure 4 shows the RIS-based SDC receiver. The emitted EM wave strikes the RIS at a carrier frequency of f_{c} and decreases downward by f_{Δ}, equivalent to $2\pi/T_{\mathrm{RIS}}$. After entering the antenna array, it passes through the band-pass filter and is amplified with low-noise amplifier (LNA). Then, it exits from the mixer and passes through the low-pass filter and finally converts to a digital baseband signal by analog-to-digital converter (ADC) [24].

3 Modeling of wireless communication system based on RIS

We introduce the general model of a RIS-based wireless communication system. This model gives an integrated framework for calculating symbol error rate (SER). The RIS-based wireless communication scheme is shown in Fig. 5, in which h_i and g_i represent the fading wireless channel coefficients or the frequency response of the wireless channel between the single-source antenna—RIS and the single-destination antenna—RIS, respectively, in non-line of sight (NLOS) mode. We have the Rayleigh fading channel model, then$h_i, g_i \sim \mathcal{CN}(0,1)$. Therefore, this model shows RIS with N simple and adjustable reflective elements in the form of a reflection array managed by control signals. There are two different performance models called consciously transmission and unaware transmission, based on knowing the RIS phase information [14, 27].

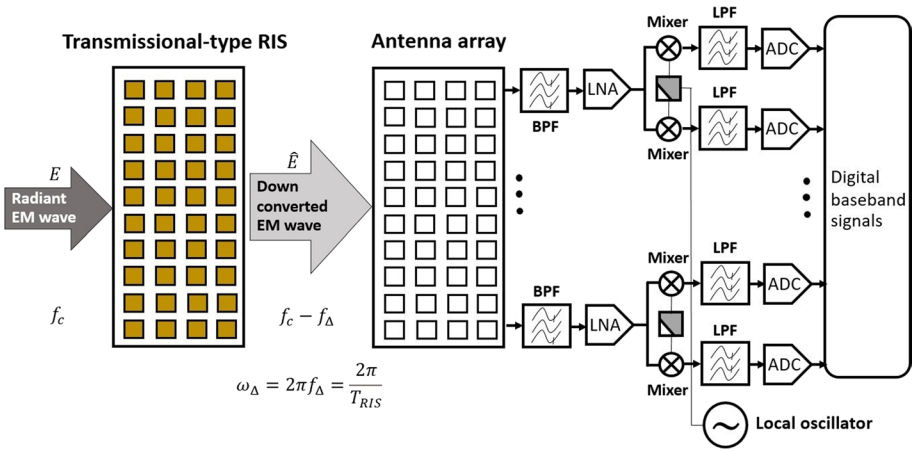

Fig.4 RIS-based SDC wireless receiver architecture

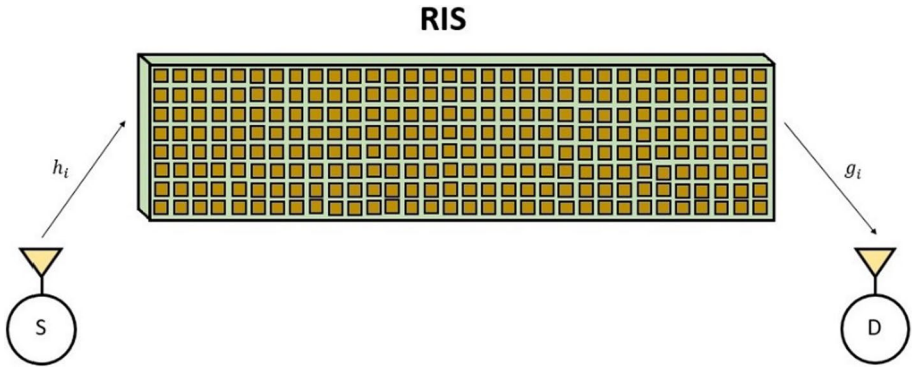

Fig.5 Using RIS for a SDC wireless communication scheme between S and D in NLOS mode

3.1 Consciously transmission via RIS-SDC

This wireless communication model works based on RIS-based SDC receiver and RIS can change or convert the radiant signal phase. In the slow flat-fading channel, the received baseband signal via RIS with the N passive element can be written as follows:

$$r = \left[\sum_{i=1}^{N} h_i e^{j\phi_i} g_i\right] x + n \tag{4}$$

where ϕ_i is the adjustable phase due to i th reflectance element of RIS, x represents the symbol sent from the M array with PSK modulation, and n is the noise in the Additive White Gaussian Noise (AWGN) model, in which $n \sim \mathcal{CN}(0, N_0)$. Therefore, the h_i and g_i in terms of amplitude and phase are expressed as:

$$h_i = \alpha_i e^{-j\theta_i} \tag{5}$$

$$g_i = \beta_i e^{-j\Psi_i} \tag{6}$$

According to Fig. 5, (4), (5), and (6), the SNR value on the receiver side is calculated as:

$$\gamma = \frac{\left|\sum_{i=1}^{N} \alpha_i \beta_i e^{j(\phi_i - \theta_i - \Psi_i)}\right|^2 E_S}{N_0} \tag{7}$$

where E_S is the average energy transmitted in each symbol, and if we want to maximize the value of γ, we must consider the phase of the RIS-based wireless channel equal to zero ($\phi_i - \theta_i - \Psi_i = 0$), i.e.,

$$\phi_i = \theta_i + \Psi_i \tag{8}$$

So, the maximum SNR value is summarized as:

$$\gamma = \frac{\left|\sum_{i=1}^{N} \alpha_i \beta_i\right|^2 E_S}{N_0} = \frac{A^2 E_S}{N_0} \tag{9}$$

It should note that α_i and β_i are Independent and Identically Distribution (I.I.D) random variables and have Rayleigh distribution, so $\mathrm{E}[\alpha_i \beta_i] = \frac{\pi}{4}$, $\mathrm{VAR}[\alpha_i \beta_i] = 1 - \frac{\pi^2}{16}$. According

to the central limit theorem (CLT) for the Gaussian random variable$A$, if we have a sufficient number of reflective elements($N \gg 10$), so $\mathrm{E}[A] = \frac{N\pi}{4}$,$\mathrm{VAR}[A] = N\left(1 - \frac{\pi^2}{16}\right)$. Thus, γ is a random variable with a Rayleigh distribution and in a decentralized Chi-square with one degree of freedom, whose moment generating function (MGF) can write as:

$$M_\gamma(s) = \left(\frac{1}{1 - \frac{sN(16-\pi^2)E_S}{8N_0}}\right)^{\frac{1}{2}} exp\left(\frac{\frac{sN^2\pi^2E_S}{16N_0}}{1 - \frac{sN(16-\pi^2)E_S}{8N_0}}\right) \tag{10}$$

In addition, the mean SNR that is proportional to N^2 can express as:

$$E[\gamma] = \frac{(N^2\pi^2 + N(16-\pi^2))E_S}{16N_0} \tag{11}$$

The average SER for the M-ary Phase Shift Keying (M-PSK) mode can also obtain:

$$P_e = \frac{1}{\pi}\int_0^{\frac{(M-1)\pi}{M}} M_\gamma\left(\frac{-\sin^2\left(\frac{\pi}{M}\right)}{\sin^2\eta}\right)\mathrm{d}\eta \tag{12}$$

which binary phase shift keying (BPSK) mode simplified as follows:

$$P_\mathrm{e} = \frac{1}{\pi}\int_0^{\frac{\pi}{2}} \left(\frac{1}{1 + \frac{N(16-\pi^2)E_S}{8\sin^2\eta N_0}}\right)^{\frac{1}{2}} exp\left(\frac{-\frac{N^2\pi^2E_S}{16\sin^2\eta N_0}}{1 + \frac{N(16-\pi^2)E_S}{8\sin^2\eta N_0}}\right) d\eta \tag{13}$$

Assuming that $\eta = \frac{\pi}{2}$, the upper bound of the error probability can express as:

$$P_\mathrm{e} \leq \frac{1}{2}\left(\frac{1}{1 + \frac{N(16-\pi^2)E_S}{8N_0}}\right)^{\frac{1}{2}} exp\left(\frac{-\frac{N^2\pi^2E_S}{16N_0}}{1 + \frac{N(16-\pi^2)E_S}{8N_0}}\right) \tag{14}$$

That is to say, RIS can turn the wireless fading channel into a great communication channel by intelligently adjusting the phase of the reflectors, which can supply very low BER values with very low SNR levels. Assuming that $\frac{NE_S}{N_0} \ll 10$, the following relation can conclude:

$$P_\mathrm{e} \propto exp\left(-\frac{N^2\pi^2E_S}{16N_0}\right) \tag{15}$$

As a result of (14), it shows the proper performance of BER in the RIS-based design because, in this part, the SNR value is comparatively low due to the exponential relationship with N^2, but decreases BER with increasing N [27]. Also, with the assumption $\frac{NE_S}{N_0} \gg 10$, the following relation can express:

$$P_\mathrm{e} \propto \left(\frac{N(16-\pi^2)E_S}{8N_0}\right)^{-\frac{1}{2}} \exp\left(-\frac{N\pi^2}{2(16-\pi^2)}\right) \tag{16}$$

It shows the performance of the BER saturation state for high SNR values due to the power relationship $(-\frac{1}{2})$. At the same time, the mean BER decreases exponentially for N and P_e increases considerably with increasing N that is reduced significantly. Using the MGF for the received SNR and $M_\gamma(s)$ we can also achieve the mean SER in M-PSK as follows:

$$P_e = \frac{4}{\pi}\left(1-\frac{1}{\sqrt{M}}\right)\int_0^{\pi/2} M_\gamma\left(\frac{-3}{2(M-1)sin^2\eta}\right)d\eta - \frac{4}{\pi}\left(1-\frac{1}{\sqrt{M}}\right)\int_0^{\pi/4} M_\gamma\left(\frac{-3}{2(M-1)sin^2\eta}\right)d\eta \tag{17}$$

Assuming that $\eta = \frac{\pi}{2}$ and $\eta = \frac{\pi}{4}$ in (17), the upper bound value for the mean SER is obtained. Assuming that $\frac{NE_S}{N_0} \ll 10$, the following relation can conclude [27]:

$$P_e \propto exp\left(-\frac{3N^2\pi^2 E_S}{32(M-1)N_0}\right) \tag{18}$$

3.2 Unaware transmission via RIS-SDC

In this case, the channel phase information (θ_i, Ψ_i) is not available, and as a result, these channel phase components cannot omit to maximize the received SNR. Without losing the generality of the theorem for $i = 0, 1, 2, \ldots, N$. We assume $\phi_i = 0$. Therefore, the received signal can be written as:

$$r = \left[\sum_{i=1}^{N} h_i g_i\right] x + n = Hx + n \tag{19}$$

Also, according to the CLT for large N and given that $H \sim \mathcal{CN}(0,1)$, the MGF for the received SNR and $M_\gamma(s)$ can be obtained as follows:

$$M_\gamma(s) = \left(1 - \frac{sNE_S}{N_0}\right)^{-1} \tag{20}$$

According to the consciously transmission model for calculating BER in the unaware transmission model, the following equation can express:

$$P_e = \frac{1}{\pi}\int_0^{\frac{\pi}{2}} \left(\frac{1}{1+\frac{NE_S}{\sin^2\eta N_0}}\right) d\eta = \frac{1}{2}\left(1 - \sqrt{\frac{\frac{NE_S}{N_0}}{1+\frac{NE_S}{N_0}}}\right) \tag{21}$$

So that the SNR gain is N times better than the point-to-point transmission through the Rayleigh fading channels [23].

3.3 RIS-based wireless communication system in RFCF mode

We offer a new pattern of wireless communication via RIS. In other words, RIS operates as RFCF transmitter (resource) in this wireless communication scheme. In these settings, RIS can be linked to the network via a wired or fiber optic. The proposed RIS-based wireless communication block diagram is shown in Fig. 6, where

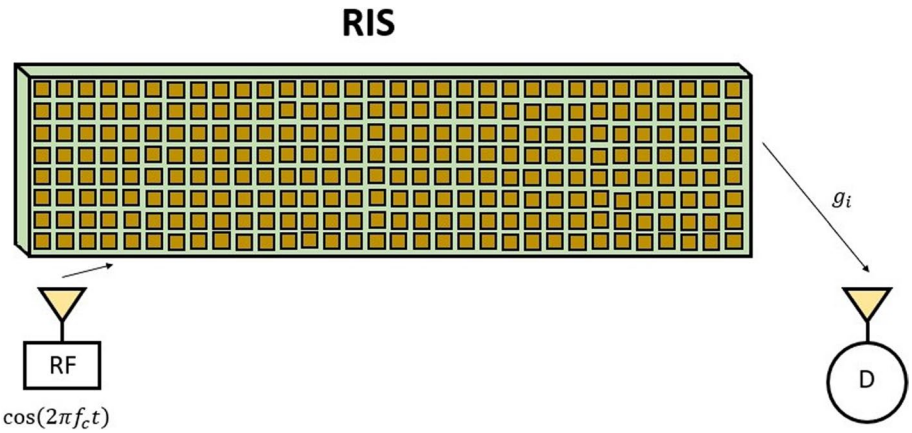

Fig.6 Wireless communication scheme via RIS-RFCF

$g_i = \beta_i e^{-j\Psi_i}$. In this scheme, the RIS supplied by the RF signal generator sends an unmodulated carrier signal $\cos 2\pi f_c$ to the RIS at a specific carrier frequency f_c. The bits are transmitted only by adjusting the phases induced by the RIS reflector. Because the channel between source and RIS is not affected by fading. Therefore, the RF signal generator must be sufficiently near to the RIS. Depending on the knowledge of the channel phase information, this model can show as a consciously transmission and unaware transmission [27].

3.3.1 Consciously transmission via RIS-RFCF

For this model, RIS adjusts the phases of its reflective elements. Not only canceling the channel phase conditions to maximize the received SNR but also correctly tuning the reflected signals on the two-dimensional plane to form a virtual M-ary signal constellation. The received signal can be written as:

$$r = \sqrt{E_S}\left[\sum_{i=1}^{N} g_i e^{j\phi_i}\right] + n \tag{22}$$

where E_S is the average energy of the transmitted signal that is not modulated and ϕ_i is the adjustable phase enforced by the i th, RIS reflector. We assume that the sum of the bits $log_2(M)$ for each signaling interval set to $\phi_i = \Psi_i + \omega_m$. By selecting the reflective phases where ω_m for $m\epsilon\{1, 2, \ldots, M\}$ the term exponential phase is commonly induced by RIS to transmit the data of the m th message. According to this issue, the received signal can be expressed as follows [21]:

$$r = \sqrt{E_S}\left[\sum_{i=1}^{N} \beta_i\right] e^{j\omega_m} + n = \sqrt{E_S} B e^{j\omega_m} + n \tag{23}$$

In addition, this signal model is similar to PSK mode in a B super-channel. Therefore, to minimize the mean SER, the phase information $\omega_1, \omega_2, \ldots, \omega_m$ of this M-PSK mode design could be chosen like the classic M-PSK mode. It can be confirmed by Conditional

Pairwise Error Probability (CPEP) for sending the message $k(\omega_k)$ and error detection as the message$l(\omega_l)$, which applies to k and l for$k, l\epsilon\{1, 2, \ldots, M\}$, so $P_{e|B}$ can calculate:

$$\begin{aligned} P_{e|B} &= P(\left|r - \sqrt{E_S}Be^{j\omega_l}\right|^2 < \left|r - \sqrt{E_S}Be^{j\omega_k}\right|^2 \\ &= P(\mathcal{R}\{r^*\sqrt{E_S}B(e^{j\omega_k} - e^{j\omega_l})\} < 0) \\ &= P(E_S B^2(1 - cos(\omega_l - \omega_k)) \\ &\quad + \mathcal{R}\{n^*\sqrt{E_S}B(e^{j\omega_k} - e^{j\omega_l})\}) < 0) = P(D < 0) \end{aligned} \tag{24}$$

Given that $D \sim \mathcal{N}(m_D, \sigma_D^2)$, $m_D = E_S B^2(1 - \cos(\omega_l - \omega_k))$, $\sigma_D^2 = N_0 E_S B^2(1 - cos(\omega_l - \omega_k))$,so we can get the followings:

$$P_{e|B} = Q\left(\sqrt{\frac{E_S B^2(1 - \cos(\omega_l - \omega_k))}{N_0}}\right) \tag{25}$$

We can minimize (25) with identically arranged phases, i.e., $\omega_m = 2\pi(m-1)/M$ for $m = 1, 2, \ldots, M$. Therefore, we have to calculate the instantaneous received SNR [21]:

$$\gamma = \frac{E_S B^2}{N_0} \tag{26}$$

According to the theorem of CLT for large N and given the Rayleigh distribution with mean $\sqrt{\pi}/2$ and variance $(4-\pi)/4$ can say to be $B \sim \mathcal{N}(m_B, \sigma_B^2)$ such that $m_B = N\sqrt{\pi}/2$ and $\sigma_B^2 = N(4-\pi)/4$. So, we have for the MGF:

$$M_\gamma(s) = \left(\frac{1}{1 - \frac{sN(4-\pi)E_S}{8N_0}}\right)^{\frac{1}{2}} exp\left(\frac{\frac{sN^2\pi E_S}{4N_0}}{1 - \frac{sN(4-\pi)E_S}{2N_0}}\right) \tag{27}$$

The mean SER of the suggested design can be obtained by substituting (27) for (12). For binary signaling, assuming that$\omega_1 = 0, \omega_2 = \pi$, the following equation can express:

$$P_e = \frac{1}{\pi}\int_0^{\frac{\pi}{2}} \left(\frac{1}{1 + \frac{N(4-\pi)E_S}{2sin^2\eta N_0}}\right)^{\frac{1}{2}} exp\left(\frac{-\frac{N^2\pi E_S}{4sin^2\eta N_0}}{1 + \frac{N(4-\pi)E_S}{2sin^2\eta N_0}}\right) d\eta \tag{28}$$

Considering $\eta = \frac{\pi}{2}$ and $\frac{NE_S}{N_0} \ll 10$, the following relation can conclude [23]:

$$P_e \propto \exp\left(-\frac{N^2\pi E_S}{4N_0}\right) \tag{29}$$

The two actual results can infer from (29). First, the suggested idea, in which RIS plays a role as a RFCF transmitter, can transmit data in ultra-reliable ways, such as the two-step RIS-SDC model presented in Fig. 5. Second, by considering (15) and (29) to obtain a purpose BER, ameliorated in desired SNR value, can be compared with the RIS-SDC model for acquired binary signaling. Therefore, in M-PSK mode, by substituting (27) for (12), we calculate the mean SER as follows:

$$P_e = \frac{1}{\pi}\int_0^{\frac{(M-1)\pi}{M}} \left(\frac{1}{1+\frac{N(4-\pi)sin^2(\frac{\pi}{M})E_S}{2sin^2\eta N_0}}\right)^{\frac{1}{2}} exp\left(\frac{-\frac{N^2\pi sin^2(\frac{\pi}{M})E_S}{4sin^2\eta N_0}}{1+\frac{N(4-\pi)sin^2(\frac{\pi}{M})E_S}{2sin^2\eta N_0}}\right) d\eta \tag{30}$$

Assuming that $\eta = \frac{\pi}{2}$ in (30), the upper bound value for the SER is obtained. Assuming that $\frac{NE_S}{N_0} \ll 10$, the following relation can conclude:

$$P_e \propto \exp\left(-\sin^2\left(\frac{\pi}{M}\right)\frac{N^2\pi E_S}{4N_0}\right) \tag{31}$$

Comparing (18) and (31), we conclude that due to the loss of SNR in M-PSK mode, some losses in the SNR for higher-order signaling ($M \geq 16$) are inevitable. However, these losses become negligible with increasing N [23].

3.3.2 Unaware transmission via RIS-RFCF

In this scenario, which is worse than previous models, RIS does not have the phase information of the Ψ_i channel and acts as a data source by aligning the phase information due to its reflection like PSK. Next, let us focus on BPSK mode, where the phases of the RIS reflector for messages 1 and 2 are set to $\phi_i = \omega_1$ and $\phi_i = \omega_2$ for all i. Therefore, the received signal can be expressed as:

$$r = \sqrt{E_S}\left[\sum_{i=1}^{N} g_i\right] e^{j\omega_m} + n = \sqrt{E_S}Ge^{j\omega_m} + n \tag{32}$$

Similar to (24), to find CPEP of the received signal for m that $m\epsilon\{1,2\}$ the following equation can be obtained:

$$P_{e|G} = Q\left(\sqrt{\frac{E_S|G|^2(1-\cos(\omega_l-\omega_k))}{N_0}}\right) \tag{33}$$

The CPEP relation also requires uniform distribution phases around the unit circle to minimize SER, which BER, like BPSK, would be optimal for binary signaling, assuming $\omega_1 = 0, \omega_2 = \pi$. Considering the CLT for large N and given $G \sim \mathcal{CN}(0,N)$. It can conclude that the instantaneous SNR of the received signal is $\gamma = \frac{E_S|G|^2}{N_0}$ obtained, and MGF is in the form $M_\gamma(s) = \left(1-\frac{sNE_S}{N_0}\right)^{-1}$. Then, by substituting it in (12) for the binary and M-ary signaling modes, the mean of SER and BER expressions is obtained as (34) and (35), respectively.

$$P_e = \frac{1}{\pi}\int_0^{\frac{(M-1)\pi}{M}} \left(\frac{1}{1+\frac{N\sin^2(\frac{\pi}{M})E_S}{\sin^2\eta N_0}}\right) \mathrm{d}\eta \tag{34}$$

$$P_e = \frac{1}{\pi}\int_0^{\frac{\pi}{2}} \left(\frac{1}{1+\frac{NE_S}{sin^2\eta N_0}}\right) d\eta = \frac{1}{2}\left(1-\sqrt{\frac{\frac{NE_S}{N_0}}{1+\frac{NE_S}{N_0}}}\right) \tag{35}$$

Table 1 Simulation settings

Parameter	Type/Value
Channel	Rayleigh fading
Modulation	M-PSK,$M\epsilon\{2, 4, 8, 16, 64\}$
Number of bits	800,000
Transmitter power	30 dBm
Noise power	10 dBm
Reflective elements	$N\epsilon\{4, 8, 16, 32, 64, 128, 256\}$
Coding	Gray
Detector	Maximum likelihood

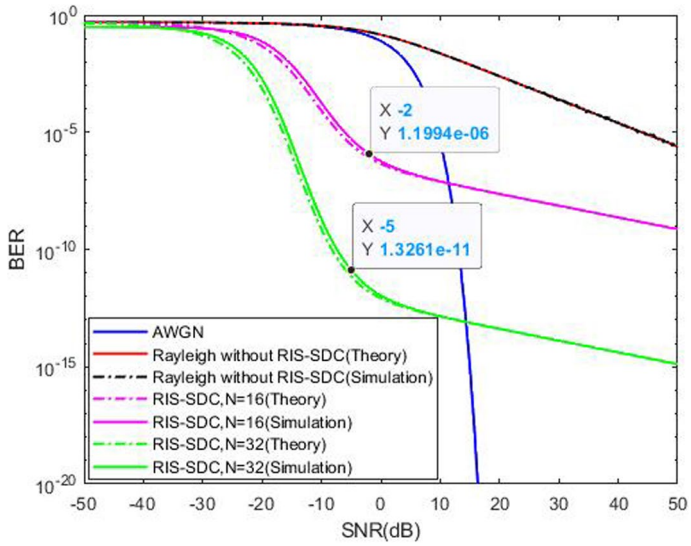

Fig.7 BER performance of RIS-SDC for $N = 16$, $N = 32$ in BPSK mode and comparison with AWGN channel and Rayleigh channel

Meanwhile, similar to the unaware RIS-SDC model, the SNR is only N times evaluated for point-to-point wireless communication over Rayleigh fading channels. It indicates that RIS also used as a RFCF transmitter only by adjusting the RIS based on the phase information [21].

4 Results and discussion

Using a computer simulation, we present the performance of the proposed models. To perform simulations, MATLAB R2019a was used. After considering the various modes, we present simulation results for a new RIS-SDC design and compare them with designs from an RIS-RFCF platform. You know the information on the channel, or you do not have access to it. In fact, all the simulations were made in consciously or unawarely mode. In our opinion, the test SNR = 20 dB, the channels as uncorrelated Rayleigh channels and E_S/N_0 is equal the SNR. Table 1 summarizes the remaining simulation parameters:

BER performance compared to SNR for $N = 16$ and $N = 32$ in the theoretical state obtained from (13) and its simulation form are drawn in Fig. 7. As it is known, the simulation form is very close to its theoretical state and the RIS-SDC scheme has better performance compared to the classic BPSK scheme of AWGN channel and Rayleigh channel in the theoretical state and its simulation mode. Also, in Rayleigh channel, the simulation form is very close to its theoretical state. It should be noted that in the Rayleigh model, the wireless connection between the source and the destination is without using RIS-SDC. As can be seen, when RIS-SDC is used, the power efficiency is much better. By comparing the different modes for the number of RIS elements, it is clear that in the RIS-SDC design, with the increase of N, its power efficiency performance improves again.

Also, according to relations (15) and (16) for $N = 16$ of the RIS-SDC scheme, for SNR $\ll -2$ dB, the BER to SNR curve is in exponential form, and for SNR $\gg -2$ dB, the BER to SNR curve is in power combination form $(-\frac{1}{2})$ and it is an exponential that reaches the saturation state with the increase of SNR. Similarly, for $N = 32$ RIS-SDC scheme, for SNR $\ll -5$ dB, the BER to SNR curve is in exponential form, and for SNR $\gg -5$ dB, the BER to SNR curve is in the form of the combination of $(-\frac{1}{2})$ power and exponential, as follows: As the SNR increases, it reaches the saturation state.

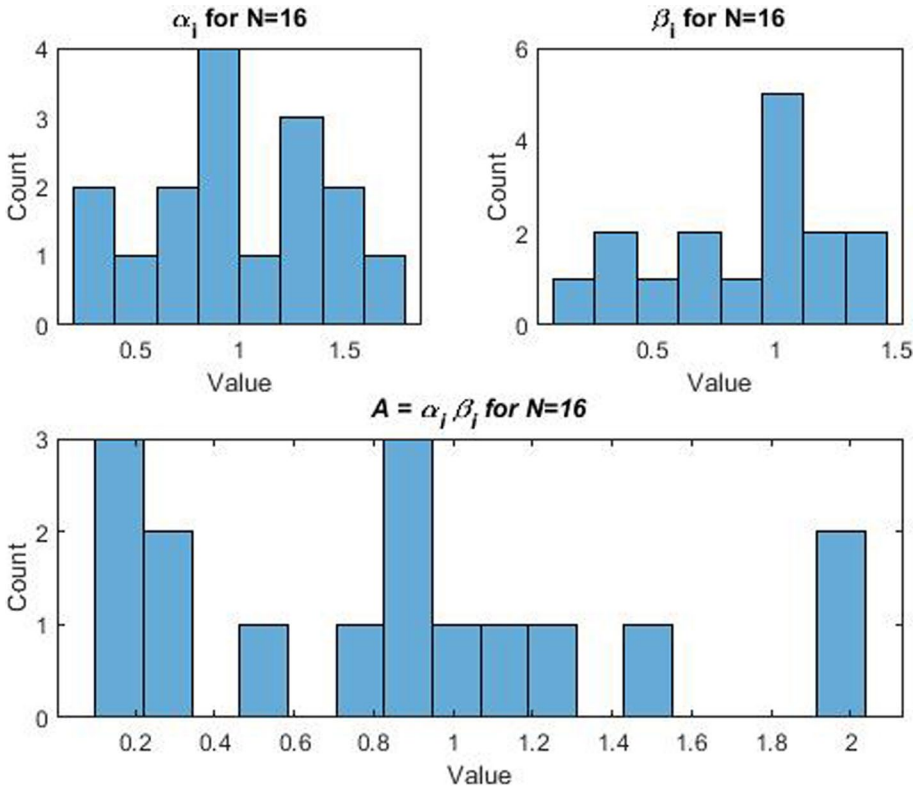

Fig.8 Histogram diagram for random variables α_i, β_i and A for $N = 16$

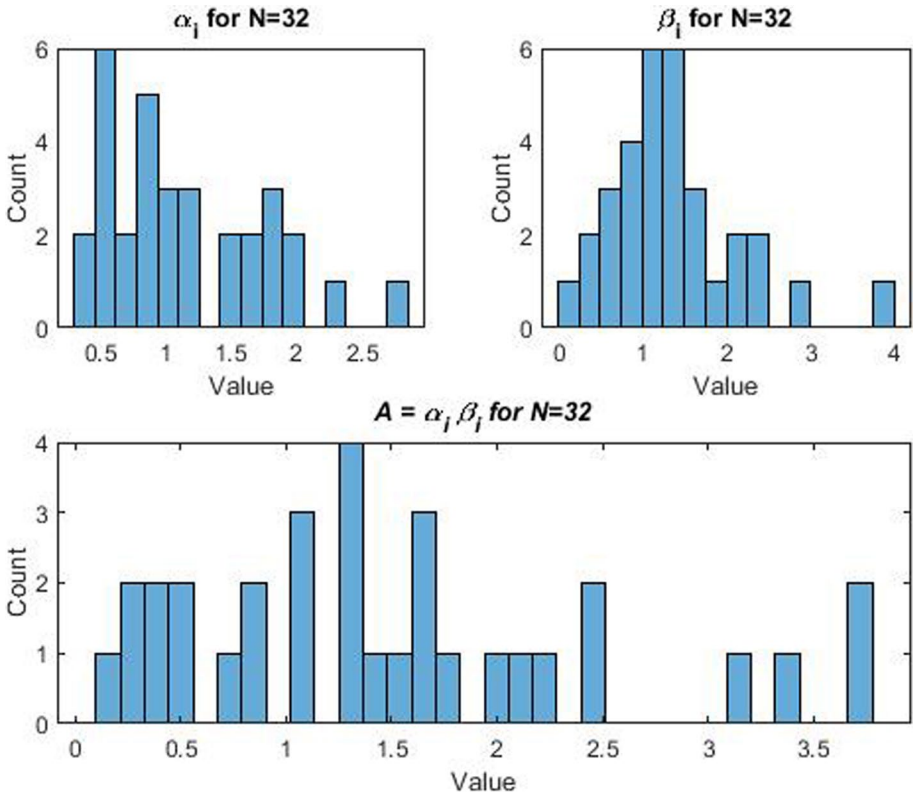

Fig.9 Histogram diagram for random variables α_i, β_i and A for $N = 16$

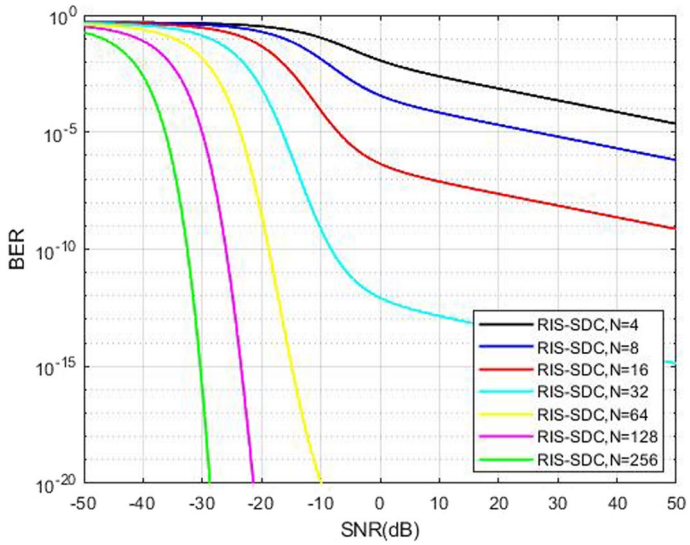

Fig.10 BER performance for RIS-SDC with different N in BPSK mode

Histograms of random variables with Rayleigh distribution α_i and β_i and random variable A with Gaussian distribution specified in (9) are drawn for $N = 16$ and $N = 32$ in Figs.8 and 9. As a result, it is clear that α_i and β_i are I.I.D random variables.

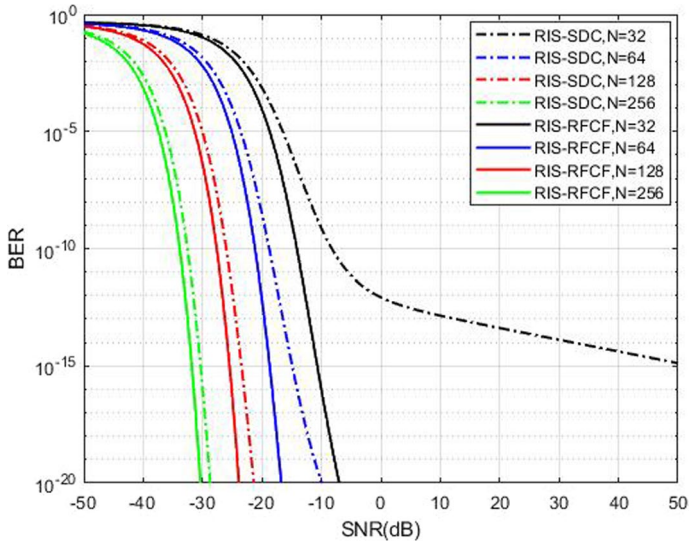

Fig.11 BER performance of RIS-SDC, RIS-RFCF with different N in BPSK mode

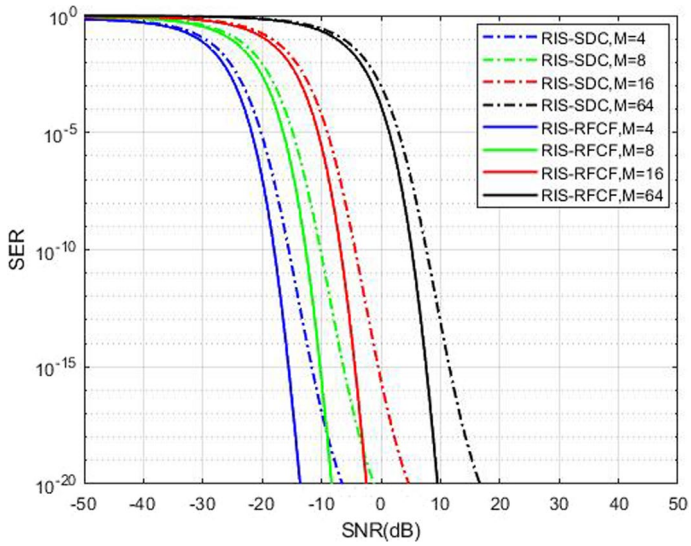

Fig.12 SER performance of RIS-SDC, RIS-RFCF for $N=64$ in M-PSK mode

BER performance of BPSK mode in RIS-SDC scheme for different N is plotted in Fig. 10. As it is shown, SNR level is reduced by approximately 12 dB by doubling N, for example from $N = 64$ to $N = 128$. Therefore, it can be said that its power efficiency performance improves.

We present BER performance of RIS-SDC and RIS-RFCF models in Fig. 11 for different N in BPSK mode. As can be seen, a RIS can be effectively used as a RFCF transmitter by preparing ultra-reliable wireless communications. Moreover, in the RIS-RFCF model, when $N=64$, the SNR can be improved by about 7 dB compared to the RIS-SDC model.

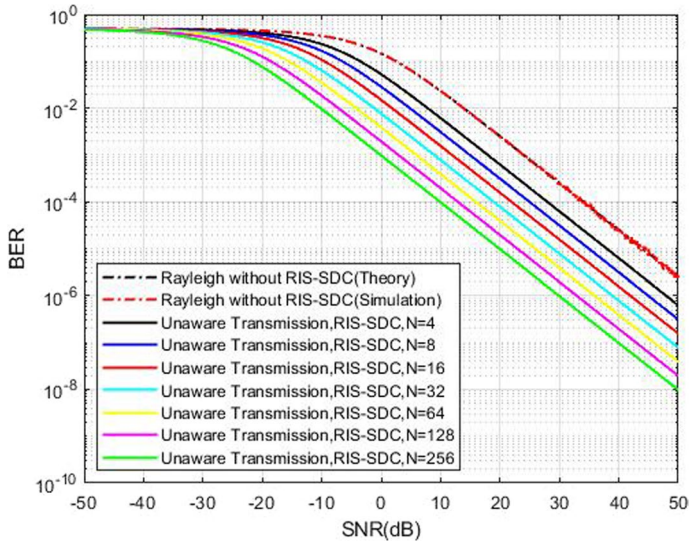

Fig.13 BER performance of RIS-SDC with different *N* in BPSK mode for unaware transmission

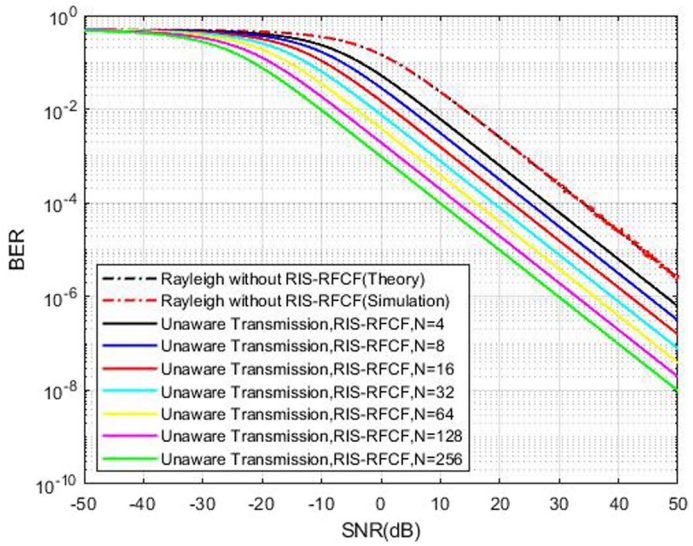

Fig.14 BER performance of RIS-RFCF with different *N* in BPSK mode for unaware transmission

SER performance of RIS-SDC and RIS-RFCF models in different M-PSK modes when $M\epsilon\{4, 8, 16, 64\}$ and the number of reflective elements is 64, shown in Fig. 12. When M as the modulation order increases in both RIS-SDC and RIS-RFCF models, SER performance deteriorates, which is more significant for ($M \geq 16$).

We show BER performance of unaware RIS-SDC and unaware RIS-RFCF designs for different N of and BPSK mode in Figs.13 and 14. In addition, both RIS-SDC and RIS-RFCF models have the same SNR distribution for unaware transmission, and doubling N prepares 3 dB betterment in needed SNR to obtain the purpose BER. However, improvements are possible by increasing N. By removing the channel phase information, the

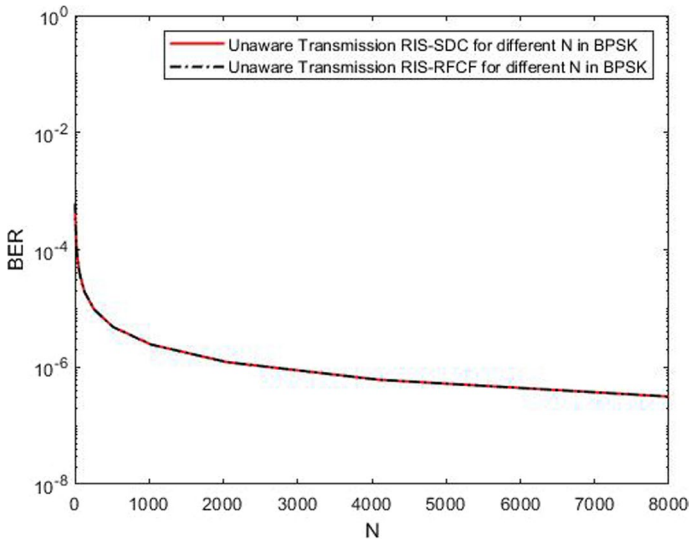

Fig.15 BER performance of RIS-SDC and RIS-RFCF for SNR = 20dB with different *N* in BPSK mode for unaware transmission

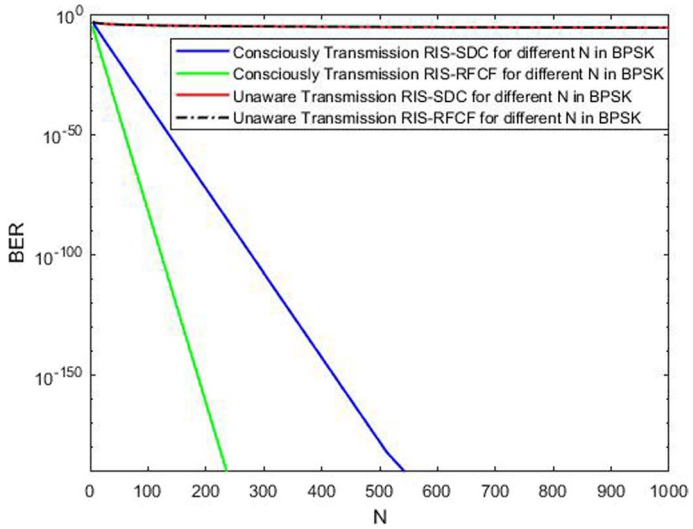

Fig.16 BER performance of RIS-SDC and RIS-RFCF for SNR = 20dB with different *N* in BPSK mode for unaware and consciously transmissions

benefits of using RIS are reduced compared to the case where we know the channel phase information, and compared to previous scenarios, the unaware RIS-SDC schemes or unaware RIS-RFCF schemes have the worst results, compared to the previous scenarios of RIS-SDC or RIS-RFCF in consciously mode. As mentioned in (21) and (35), it is also clear in Figs.13 and 14 that SNR gain is N times better than the point-to-point transmission through the Rayleigh fading channels without RIS-SDC or RIS-RFCF.

The overall BER performance for the unaware transmission system when SNR = 20 dB for RIS-SDC and RIS-RFCF models is plotted in Fig. 15. As it is known, with the increase of N, the value of BER decreases, but in the best case, it is not less than 10^{-7}.

Therefore, as previously, both in terms of theory and in terms of simulation, the power efficiency of the unaware transmission system was investigated, because we do not have the wireless channel information available, the power efficiency of this system is much lower than the consciously system.

The overall BER performance for the consciously transmission system when SNR = 20 dB for RIS-SDC and RIS-RFCF models and compared with the unaware transmission system is plotted in Fig. 16. As it is known, with the increase of N, the value of BER decreases, so that in the RIS-SDC model at $N = 512$ and in the RIS-RFCF model at $N = 256$, the BER value becomes almost zero, which shows the reliability of the system. It was also shown that by designing a system with SNR = 20 dB, a reliable system with good power efficiency can be achieved for the RIS-SDC model with 512 passive elements and for the RIS-RFCF model with 256 passive elements. Therefore, it is argued that the stated models are more efficient.

5 Conclusion

The revolutionary technologies are making significant changes to the physical layer of wireless communication systems. Nevertheless, many concepts are in the field of theoretical reconnaissance. Given the evolving technologies, immense research and progress in the physical layer require to make these technologies practical in wireless communication systems.

To realize low-cost and low-power wireless communication networks in the future, we propose two new and innovative designs called RFCF transmitter and SDC receiver, both of which based on RIS. The basic principles are architectural design and the promising benefits of these new methods presented. It also shows that due to the superior ability of RIS to change in amplitude and phase of EM waves, we may see a fundamental change in the design of wireless transmission systems. It is essential that appropriate measuring instruments are developed since research into the use of RIS in wireless communication systems has not yet been fully established. The performance of the RIS wireless transmission system depends on its design level or number of reflective elements and their production method from a RIS. Only one frequency of the carrier is taken into account by the reviewed models. Therefore, the study of how to combine RIS technologies with OFDM-MIMO should be initiated.

We evaluated the potential of RIS to contribute to future wireless communications in terms of good BER and SNR performance using mathematical modeling. From the simulation results, it can be concluded that RIS-based transmission can effectively enhance the received SNR, and extremely reliable communication (low error probability) can be achieved with very low SNR values. In other words, improved power efficiency in future wireless networks can be achieved with the help of reconfigurable intelligent surfaces. We have also shown that, with a very simple architecture, RIS can be used as a RFCF transmitter for the f_c carrier frequency. The submitted RIS-RFCF model is more efficient than the revised RIS-SDC model when it comes to power efficiency. Therefore, it is argued that the models at issue are more efficient. We will assume a SNR of 20dB if we have any information about the wireless channel. It is possible to conclude that the 512 elements RIS-SDC and 256 elements RIS-RFCF models, thanks to their assistance from

RIS, will achieve optimum state of power efficiency and high reliability in wireless communication modelling.

Finally, it can be concluded that the effective use of RIS may create changed methods in 6G wireless networks, so it is suggested that in the case of IM-based schemes, correlated channels, different types of fading, different types of interference, investigating the effects of the Doppler phenomenon and the resulting frequency shift will appear as interesting topics in the future research of wireless communication.

Abbreviations

5G	Fifth generation
OFDM	Orthogonal frequency division multiplexing
B5G	Beyond fifth generation
NOMA	Non-orthogonal multiple access
VLC	Visible light communication
UM-MIMO	Ultra-massive multi-input multi-output
6G	Sixth generation
RIS	Reconfigurable intelligent surfaces
QoS	Quality of service
RF	Radio-frequency
RFCF	Radio-frequency chain free
SDC	Space down-conversion
MIMO	Multi-input multi-output
BER	Bit error rate
SNR	Signal-to-noise ratio
EM	Electro-magnetic
PA	Power amplifier
LPF	Low-pass filter
BPF	Band-pass filter
DAM	Direct antenna modulation
OOK	On–off keying
FSK	Frequency shift keying
DPSM	Direct phase shifter modulation
DAC	Digital-to-analog converter
PSK	Phase shift keying
LNA	Low-noise amplifier
ADC	Analog-to-digital converter
SER	Symbol error probability
NLOS	Non-line of sight
AWGN	Additive white Gaussian noise
I.I.D	Independent and identically distributed
CLT	Central limit theorem
MGF	Moment generating function
M-PSK	M-ary phase shift keying
BPSK	Binary phase shift keying
CPEP	Conditional pairwise error probability

Acknowledgements
Not applicable.

Author contributions
All authors have reviewed and edited the manuscript and have approved the final manuscript.

Funding
Not applicable.

Availability of data and materials
All results are included in this published article; the results raw output is available from the corresponding author on reasonable request.

Declarations

Competing interests
The authors declare that they have no competing interests.

Received: 13 June 2022 Accepted: 2 April 2024
Published online: 29 May 2024

References

1. X. Cao, P. Yang, M. Alzenad, X. Xi, D. Wu, H. Yanikomeroglu, Airborne Communication Networks. IEEE J. Select. Areas Commun. **36**(9), 1907–1926 (2018)
2. H. Murata, N. Kohmu, Y.N. Wijayanto, Y. Okamura, Integration of patch antenna on optical modulators. IEEE Photon. Soc. Newslett. **28**(2), 4–7 (2014)
3. T. Nagatsuma, G. Ducournan, C.C. Renaud, Advances in terahertz communications accelerated by photonics. Nat. Photon. J. **10**(6), 371–379 (2016)
4. Y. Yuan, Z. Yuan, L. Tian, 5G non-orthogonal multiple access study in 3GPP. IEEE Wirel. Commun. Mag. **58**(7), 90–96 (2020)
5. F. Tariq, M.R.A. Khandaker, K.-K. Wong, M.A. Imran, M. Bennis, M. Debbah, A speculative study on 6G. IEEE Wirel. Commun. **27**(4), 118–125 (2020)
6. C. Han, J. M. Jornet, and I. F. Akyildiz, Ultra-Massive MIMO Channel Modeling for Graphene-Enabled Terahertz-Band Communications, in *IEEE 87th Vehicular Technology Conference (VTC Spring)*, pp. 1–5, (2018)
7. T. J. Cui, S. Liu, L. Zhang, Information metamaterials and metasurfaces, in *IEEE 43th International Conference on Infrared, Millimeter, and Terahertz Waves (IRMMW-THz)*, pp.3644–3668, (2018)
8. W. Yao, Y. Wang, Direct antenna modulation–a promise for ultra-wideband (UWB) transmitting, in *IEEE MTT-S Int. Microwave Symposium Digest*, pp. 1273–1276, (2004)
9. M.P. Daly, E.L. Daly, J.T. Bernhard, Demonstration of directional modulation using a phased array. IEEE Trans. Antennas Propag. **58**, 1545–1550 (2010)
10. W. Tang et al., Wireless communications with programmable metasurface: transceiver design and experimental results. IEEE Wirel. Commun. **27**(2), 180–187 (2020)
11. M.D. Renzo et al., Smart radio environments empowered by reconfigurable AI meta-surfaces: an idea whose time has come. EURASIP J. Wirel. Commun. Netw. **129**, 529–541 (2019)
12. M.T. Nouman et al., Vanadium dioxide based frequency tunable metasurface filters for realizing reconfigurable terahertz optical phase and polarization control. Opt. Express J. **26**(10), 12922–12929 (2018)
13. E. Seifi, M. Atamanesh, A. K. Khandani, Media-based MIMO: Outperforming Known Limits in Wireless, in *IEEE International Conference on Communications (ICC)*, pp 1–7, (2016)
14. E. Basar, media-based modulation for future wireless systems: a tutorial. IEEE Wirel. Commun. **26**(5), 160–166 (2019)
15. Y. Ding, V. Fusco, A. Shitvov, Y. Xiao, H. Li, Beam index modulation wireless communication with analog beamforming. IEEE Trans. Veh. Technol. **67**(7), 6340–6354 (2018)
16. L. Subrt, P. Pechac, Controlling propagation environments using intelligent walls, in *6th European Conference on Antennas Propagation (EUCAP)*, pp. 1–5, (2012)
17. S. Hu, F. Rusek, O. Edfors, Beyond massive MIMO: the potential of data transmission with large intelligent surfaces. IEEE Trans. Signal Process. **66**(10), 2746–2758 (2018)
18. Q. Wu, R. Zhang, Intelligent Reflecting Surface Enhanced Wireless Network: Joint Active and Passive Beamforming Design, in *IEEE Global Communication Conference* (2018)
19. C. Huang, A. Zappone, G.C. Alexandropoulos, M. Debbah, C. Yuen, Reconfigurable intelligent surfaces for energy efficiency in wireless communication. IEEE Trans. Wireless Commun. **18**(8), 4157–4170 (2019)
20. E.C. Strinati et al., 6G: The next frontier: from holographic messaging to artificial intelligence using sub-terahertz and visible light communication. IEEE Veh. Technol. Mag. **14**(3), 42–50 (2019)
21. E. Basar, Transmission Through Large Intelligent Surfaces: A New Frontier in Wireless Communications, in *European Conference on Networks and Communications (EuCNC)*, pp 112–117, (2019)
22. Q. Wu, R. Zhang, Towards smart and reconfigurable environment: intelligent reflecting surface aided wireless network. IEEE Commun. Mag. **58**(1), 106–112 (2020)
23. E. Basar, M. Di Renzo, J. De Rosny, M. Debbah, M. Alouini, R. Zhang, Wireless communications through reconfigurable intelligent surfaces. IEEE Access **7**, 116753–116773 (2019)
24. W. Tang et al., Wireless communications with programmable metasurface: new paradigms, opportunities, and challenges on transceiver design. IEEE Wirel. Commun. **27**(2), 180–187 (2020)
25. A. Amiri, M. Angjelichinoski, E. de Carvalho, R. W. Health, Extremely Large Aperture Massive MIMO: Low Complexity Receiver Architectures, in *2018 IEEE Global Communications Conference Workshop*, pp. 1–6, (2018)
26. L. Zhang et al., Space-time-coding digital metasurfaces, in *IEEE 13th International Congress on Artificial Materials for Novel wave Phenomena (Metamaterials)*, pp 128–130, (2019)
27. E. Basar, M. Wen, R. Mesleh, M.D. Renzo, Y. Xiao, H. Haas, Index modulation techniques for next-generation wireless networks. IEEE Access **5**, 16693–16746 (2017)
28. B. Zong et al., 6G technologies. IEEE Veh. Technol. Mag. **14**(3), 18–27 (2019)
29. K. David, H. Berndt, 6G vision and requirements. IEEE Veh. Technol. Mag. **13**(3), 72–80 (2018)
30. Y. Huo, X. Dong, W. Xu, M. Yuen, Enabling multi-functional 5G and beyond user equipment: a survey and tutorial. IEEE Access **7**, 116975–117008 (2019)
31. J.M. Jornet, I.F. Akyildiz, Graphene-based plasmonic nano-antenna for terahertz band communication in nanonetworks. IEEE J. Sel. Areas Commun. **31**, 685–694 (2013)
32. Y. Ren et al., Line-of-sight millimeter-wave communications using orbital angular momentum multiplexing combined with conventional spatial multiplexing. IEEE Trans. Wirel. Commun. **16**(5), 3151–3161 (2017)
33. S. Bhattarai, J.M. Park, B. Gao et al., An overview of dynamic spectrum sharing: ongoing initiatives, challenges, and a roadmap for future research. IEEE Trans. Cognit. Commun. Netw. **2**(2), 110–128 (2017)
34. S. Han, T. Xie, C.-L. I, Greener physical layer technologies for 6g mobile communications. IEEE Commun. Mag. **59**(4), 68–74 (2021)
35. V.F. Fusco, Q. Chen, Direct-signal modulation using a silicon microstrip patch antenna. IEEE Trans. Antennas Propag. **47**(6), 1025–1028 (1999)
36. M. Salehi, M. Manteghi, S.-Y. Suh, S. Sajuyigbe, H.G. Skinner, A Wideband frequency-shift keying modulation technique using transient state of a small antenna. IEEE Trans. Antennas Propag. **94**, 1421–1445 (2016)

37. W. Tang et al., Programmable metasurface-based RF chain-free 8PSK wireless transmitter. Electron. Lett. J. **55**(7), 417–420 (2019)
38. Y. Zeng, R. Zhang, Millimeter wave MIMO with lens antenna array: a new path division multiplexing paradigm. IEEE Trans. Commun. **64**(4), 1557–1571 (2016)
39. Y. Naresh, A. Chockalingam, On media-based modulation using RF mirrors. IEEE Trans. Veh. Technol. **66**(6), 4967–4983 (2017)
40. Y. Ding, K.J. Kim, T. Koike-Akino, M. Pajovic, P. Wang, P. Orlik, Spatial scattering modulation for uplink millimeter-wave systems. IEEE Commun. Lett. **21**(7), 1493–1496 (2017)
41. C. Liaskos, S. Nie, A. Tsioliaridou, A. Pitsillides, S. Ioannidis, I. Akyildiz, A new wireless communication paradigm through software-controlled metasurfaces. IEEE Commun. Mag. **56**(9), 162–169 (2018)
42. X. Tan, Z. Sun, J. M. Jornet, D. Pados, Increasing indoor spectrum sharing capacity using smart reflect-array, in *IEEE International Conference on Communications (ICC)*, pp 1–6, (2016)
43. C. Huang, A. Zappone, M. Debbah, C. Yuen, Achievable Rate Maximization by Passive Intelligent Mirrors, in *IEEE International Conference on Acoustics and Speech Signal Processing (ICASSP)*, pp 3714–3718, (2018)
44. C. Huang, G. C. Alexandropoulos, A. Zappone, M. Debbah, C. Yuen, Energy Efficient Multi-User MISO Communication using Low Resolution large intelligent Surfaces, in *IEEE Global Communication Conference*, (2018)
45. Q. Wu, R. Zhang, Beamforming Optimization for Intelligent Reflecting Surface with Discrete Phase Shifts, in *IEEE International Conference on Acoustics, Speech and Signal Processing (ICASSP)*, pp 7830–7833, (2019)
46. A. Mahmoudi Rad, J. Pourrostam, M.A Tinati, Improve power efficiency in 6g wireless communications through reconfigurable intelligent surfaces, in 5th Iranian Conference on Communications Engineering (ICCE). pp. 153–157, (2021). https://civilica.com/doc/1328609/

Publisher's Note

Amin Mahmoudi Rad received the B.Sc. degree in electrical engineering-telecommunications from the Islamic Azad University of Urmia, Urmia, Iran, in 2007, and the M.Sc. degree in communication systems engineering from the University of Tabriz, Iran, in 2023. His research interests include wireless communication systems and signal processing for communication systems.

Jafar Pourrostam received the B.Sc. degree in electronic engineering from the Amir Kabir University of Technology, Tehran, Iran, in 2000, the M.Sc. degree in communication systems engineering from the University of Tehran, Iran, in 2003, and the Ph.D. degree in electrical engineering from Michigan Technological University, USA, in 2007. He was with the Research and Development Department, PCTEL, a leading global provider of wireless technology solutions, from 2008 to 2013. He is currently an Associate Professor at the Department of Electrical and Computer Engineering, University of Tabriz, Iran. His research interests include wireless communications, mobile communication systems and signal processing.

Mohammad Ali Tinati received the B.Sc. degree in electrical engineering-telecommunications from Northeastern University, Boston, USA, in 1977, the M.Sc. degree in the M.Sc. degree in electrical engineering-telecommunications from Northeastern University, Boston, USA, in 1978, and the Ph.D. degree in biomedical signal processing from University of Adelaide, Adelaide, Australia, in 1999. Professor at the department of electrical and computer engineering, University of Tabriz, Iran. His research interests include digital signal processing, biomedical signal processing, adaptive systems, wavelet transform, speech processing, time–frequency analysis, sensor networks and hardware for signal processing.